8th International Symposium on Magnetic Bearing
August 26-28, 2002, Mito, Japan

# ACHIEVING ULTRA-HIGH ROTATING SPEEDS

**A. R. Boletis, H. Bleuler**
Laboratoire de Systèmes Robotiques, EPFL, 1015 Lausanne, Switzerland
alexis.boletis@epfl.ch
hannes.bleuler@epfl.ch

**ABSTRACT**
Some experiments were made in the past in order to produce high centrifugal fields by spinning little spherical rotors. In particular, J. Beams investigated the production of high centrifugal fields and in 1946 he obtained a centrifugal field of $2.4 \times 10^8$ G by spinning a 0.795 [mm] diameter solid steel ball-bearing ball in vacuum. The work presented in this paper is based on J. Beams experiments. A small device was realized to actively stabilize one degree of freedom of a sub-millimetric spherical rotor and to spin it. Small spherical rotors with diameter down to 0.5 [mm] have been levitated and driven by an induction motor.

## INTRODUCTION

High speed rotation of small rotors is needed more and more in many industrial applications. Classical examples are turbines, spindles, flywheels. Compact devices can be used for scanners, gyroscopes, centrifuge units, spinning rotor gauges and for microtechnology materials testing.

The centrifugal field obtained in 1946 by J. Beams with a 0.795 [mm] diameter spherical rotor corresponds to $23.16 \times 10^6$ rpm and it is the actual record of rotating speed [1]. There are many difficulties to achieve ultra-high rotating speed, and the publications do not describe in detail the complex installation used for his experiences. To our knowledge, nobody else has published further research in this field.

Our goal is to develop and to realize a small optimized device in order to reproduce J.Beams experiences and to levitate and spin even smaller rotors.

## ROTOR STRESS UNDER CENTRIFUGAL LOAD

Geometry and mechanical properties of the rotor will determine the maximum achievable speed. If this speed is exceeded, the rotor will burst under centrifugal stresses. The maximum peripheral speed for a given shape of rotor is constant [2] and depends essentially on the yield strength-to-density ratio. Therefore decreasing the rotor diameter, the maximum achievable rotating speed will increase (1).

$$v_{p,\,max} = \omega_{max} \cdot r \qquad (1)$$

where $v_{p,max}$ is the maximum peripheral speed and $\omega_{max}$ is the maximum rotating speed with a given rotor diameter $r$.

Analytical equations for stresses in a full disc rotor have been established [3, 4]. For example, $v_{p,max}$ for a steel rotor is 576 [m/s], while for an amorphous metal rotor is 826 [m/s]. An interesting result is that for a disc with a center hole, the maximum peripheral speed is decreased by a factor of $1/\sqrt{2}$ compared to a full disc rotor.

The maximum measured rotating speed, reported by J. Beams in 1946, corresponds to a $v_{p,max}$ of 965 [m/s]. This value of maximum peripheral speed seems to be too high compared to those given above. Thus, some considerations have to be made regarding to this result. Rotors of small dimensions have less defects than big rotors, therefore yield strength can be higher than nominal value given by material manufacturers. Moreover, the spherical shape of the rotor will introduce shear stress and its maximum peripheral speed will therefore be higher compared to a cylindrical shape.

## THE DEVICE

The small device that was realized is composed of two optical sensing systems for the rotor position and its speed, a single vertical magnetic actuator and a two-phase induction motor with ferrite cores (figures 1,2). The magnetic actuator vertically stabilizes the rotor, while horizontal stabilization is passive. Analog control is used. Spherical rotors with diameters up to 1 [mm] can be levitated and spun.

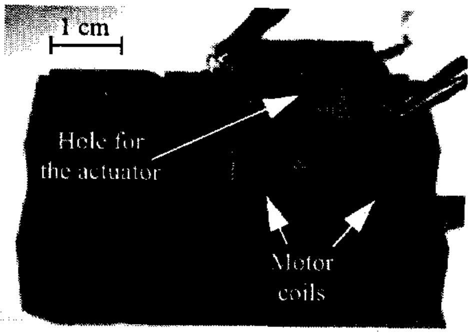


**FIGURE 1:** The device

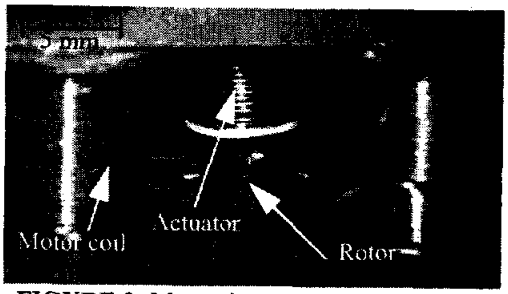


**FIGURE 2:** Magnetic actuator and motor coils

### Magnetic Actuator

Levitation of the rotor and stabilization of its vertical position is performed with an actively controlled single magnetic actuator (figure 3).

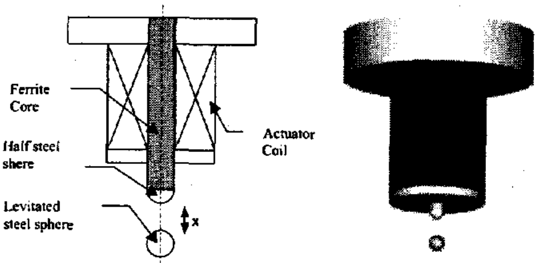


**FIGURE 3:** Schematic and 3D view of the actuator

Horizontal centering and stabilization of the rotor is passive, and it is ensured by the shape of the end of the actuator core and by the gyroscopic effect, during spinning.

**Model.** The magnetic force of the actuator depends on the rotor vertical position and the current injected in the actuator coil. It is derived from the magnetic energy and, since the current $i$ injected is controlled and therefore known, the only unknown variable is the inductance L (2).

$$F_{mag}(x) = \frac{1}{2} \cdot \frac{dL(x)}{dx} \cdot i^2 \qquad (2)$$

The inductance L can be approximated by the following empirical expression (3):

$$L(x) = L_0 + \frac{\Delta L}{1 + a \cdot x} \qquad (3)$$

where $L_0$ is the inductance of the actuator coil without the rotor, $\Delta L$ is the maximum variation of the coil inductance (figure 4), $a$ is a fitting parameter and $x$ is the distance between the rotor and the end of the actuator. The curve $L(x)$ is obtained experimentally and the parameters are identified.

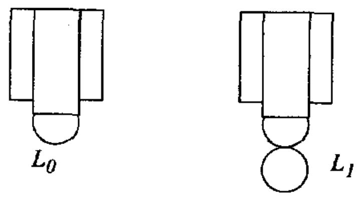


$$\Delta L = L_1 - L_0$$

**FIGURE 4:** Maximum variation of the coil inductance

For a given air gap $x_0$, we can obtain the bias current needed to compensate the weight m of the rotor (4).

$$i_b = (1 + a \cdot x_0) \cdot \sqrt{\frac{2 \cdot m \cdot g}{a \cdot \Delta L}} \qquad (4)$$

After linearization at the equilibrium point of the magnetic force, the parameters $k_x$ and $k_i$ are given by (5) and (6).

$$k_x = \frac{i_b^2 \cdot a^2 \cdot \Delta L}{(1 + a \cdot x_0)^3} \qquad (5)$$

$$k_i = \frac{i_b \cdot a \cdot \Delta L}{(1 + a \cdot x_0)^2} \qquad (6)$$

**Position Sensing System**
Because of its insensibility towards magnetic fields, an optical sensing system is used to measure the rotor vertical position. It is composed of a laser source and a four segments photodiode (figure 5).

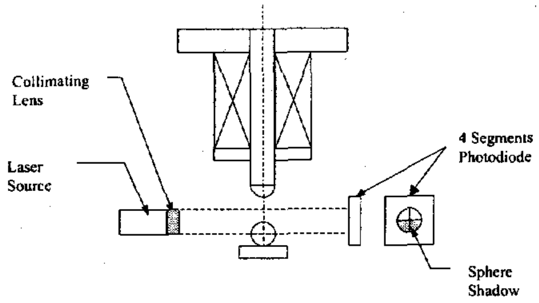


**FIGURE 5:** Position sensing principle

A red laser source with an integrated collimating lens illuminates the rotor. The shadow of the rotor is detected by the four segments photodiode, placed behind it.
The vertical displacement $x$ of the rotor can be obtained with the expression shown in figure 6.

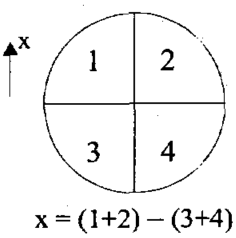


**FIGURE 6:** 4 segments photodiode - displacement x

A signal conditioning card carries out the simple operation on the 4 segments and amplifies the output signal.

**Controller**
The controller is an analog PD controller. It was synthesized from the parameters $k_i$, $k_x$, the sensor sensitivity and the amplifier gain.

**Motor**
To achieve ultra-high rotating speed, high frequency and high power driving electronics are needed. Moreover, motor iron losses become important and the skin effect appears in the coils wires producing non-desirable heating.
In order to keep the excitation as low as possible frequency of the current, a two-phase (90° shifted) induction motor with an minimum of two poles per phase was designed and realized. It is composed of four coils, with ferrite as core material, so that eddy currents losses are reduced (figure 7).

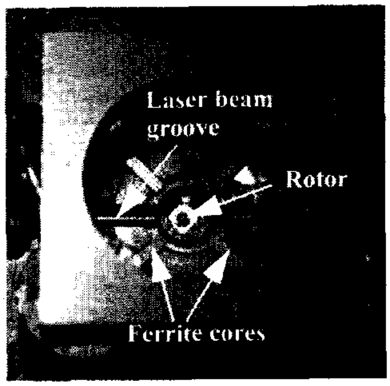


**FIGURE 7:** Top view of the motor

Since there is no active control for the horizontal centering of the rotor, the air gap of the motor has to be calculated in order not to destabilize the rotor (figure 8).

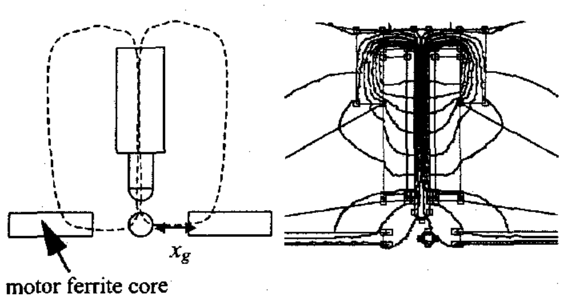


**FIGURE 8:** Influence of the motor air gap

Finite element simulations have shown that a motor air gap $x_g$ at least three times higher than the magnetic bearing air gap is sufficient to preserve stability of the rotor around the working position.

The driving electronics to create the high speed rotating magnetic field is composed of two PWM drivers with an integrated H-bridge, which can supply up to 2A at a maximum switching frequency of 250 kHz.

**Rotating Speed Measurements**
The speed measurement principle is also optical. A photodiode is placed under the rotor. The laser source is the same used for position sensing. When the surface reflectivity of the rotor is not uniform (one half is darkened), during spinning, the photodiode detects an intensity variation which correspond to the rotating frequency (figure 9). In order to have a maximum intensity variation, a well defined rotation axis has to be guaranteed.

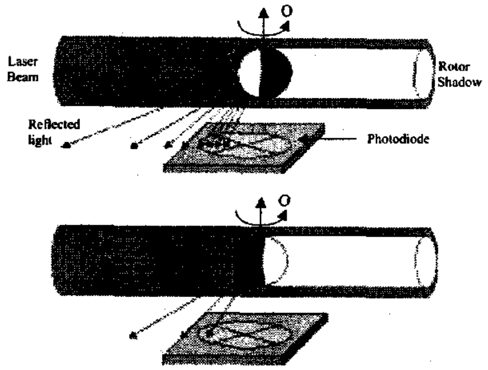


**FIGURE 9:** Speed measurement principle

## RESULTS

Stable levitation was achieved with 0.5 [mm] and 1 [mm] diameter rotors. Rotation tests were made with a 1 [mm] diameter rotor to facilitate speed measurements. Adhesion forces between the support and the small rotors become not negligible, therefore a frequent clean up is needed to obtain a repeatable stable levitation. Table 1 summarizes magnetic bearing characteristics for a 1 [mm] diameter rotor.

**TABLE 1:** Magnetic bearing characteristics

| | |
|---|---|
| $L_0$ | 430 [μH] |
| $x_0$ | 300 [μm] |
| $i_b$ | 270 mA |
| $k_i$ | $3 \cdot 10^{-4}$ [N/A] |
| $k_x$ | 0.22 [N/m] |
| sensor sensitivity | 56 [V/mm] |
| sensor working range | 0.6 [mm] |
| sensor resolution | 700 [nm] |
| rotor mass | 4.1 [mg] |

Table 2 summarizes principal characteristics of the induction motor.

**TABLE 2:** Motor characteristics

| | |
|---|---|
| Phases | 2 |
| Phase resistance | 64 [mΩ] |
| Phase inductance | 31 [μH] |
| Supply voltage | 0-50 [V] |
| Operating frequency | 100 [kHz] |
| $x_g$ | 2.5 [mm] |

Rotating speed was measured for different supply voltages and the results are shown in figure 10.

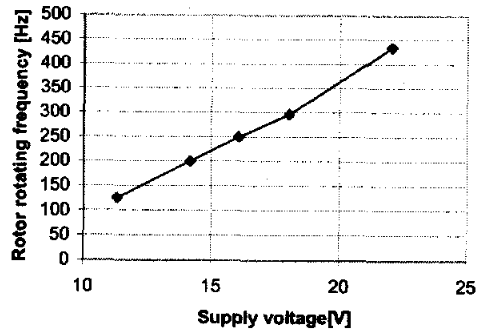


**FIGURE 10:** Motor performance at 100 kHz

The maximum speed achieved with this device at normal conditions (1 atm, 25°C) is 60'000 rpm. It is probably possible to obtain a higher rotating speed, but at the moment the most important difficulty is to pass radial critical speeds (from 20'000 to 60'000 rpm). No horizontal damping is present and strong radial vibration of the rotor occurs.

## CONCLUSIONS AND OUTLOOK

A new small device to levitate and to spin small spherical rotors up to 1 [mm] diameter was design and realised. The rotor speed measurement system was also integrated. Levitation and rotation up to 60'000 rpm was successfully achieved with 1 [mm] diameter rotors.
Further improvements of the device will be three degrees of freedom active control in order to damp horizontal vibrations. Speed measurement improvement will be based on the detection of the unbalance of the rotor. Finally, rotor stresses and deformations have to be carefully investigated to estimate bursting speed of the rotor.

## REFERENCES


1. J. W. Beams, J. L. Young, III, and J. W. Moore, The Production of High Centrifugal Fields, Journal of applied physics, 1946, pp. 886-890
2. J. W. Beams, Magnetic Suspension for Small Rotors, The Review of Scientific Instruments, Vol. 21, No. 2, 1950, pp. 182-184
3. R. Larsonneur, Design and Control of Active Magnetic Bearing Systems for High Speed Rotation, Diss. ETH No. 9140, Zürich, 1990
4. G. Schweitzer, H. Bleuler, A, Traxler, Active Magnetic Bearings, Zürich, 1994, ISBN 3 7281 2132 0